THE JOURNAL OF PHYSICAL CHEMISTRY Letters

pubs.acs.org/JPCL

Reliable Formation of Single Molecule Junctions with Air-Stable Diphenylphosphine Linkers

R. Parameswaran,[†] J. R. Widawsky,[‡] H. Vázquez,[§] Y. S. Park,[§,∥] B. M. Boardman,[§,∥] C. Nuckolls,[§,∥] M. L. Steigerwald,[§,∥] M. S. Hybertsen,*[,⊥] and L. Venkataraman*[,‡,§]

[†]Department of Chemistry and Physics, Barnard College, New York, New York, 10027, [‡]Department of Applied Physics and Applied Mathematics, [§]Center for Electron Transport in Molecular Nanostructures, and [∥]Department of Chemistry, Columbia University, New York, New York, 10027, and [⊥]Center for Functional Nanomaterials, Brookhaven National Laboratory, Upton, New York, 11973

ABSTRACT We measure the conductance of single Au−molecule−Au junctions with a series of air-stable diphenylphosphine-terminated molecules using the scanning tunneling microscope-based break junction technique. Thousands of conductance versus displacement traces collected for each molecule are used to statistically analyze junction conductance and evolution upon elongation. Measured conductances for a series of alkane-based molecules exhibit an exponential decrease with increasing length, as expected for saturated molecules, with a tunneling decay constant of 0.98 ± 0.04. Measurements of junction elongation indicate strong metal−molecule binding, with a length that increases with the number of methylene groups in the backbone. Measured conductance histograms for four molecules with short, unsaturated backbones (e.g., benzene) are much broader with less well-defined peaks. These measurements are supported by density function theory calculations. The phosphine binds selectively to under-coordinated gold atoms through a donor−acceptor bond with a binding energy of about 1 eV. The calculated tunnel coupling correlates very well with experiment.

SECTION Electron Transport, Optical and Electronic Devices, Hard Matter

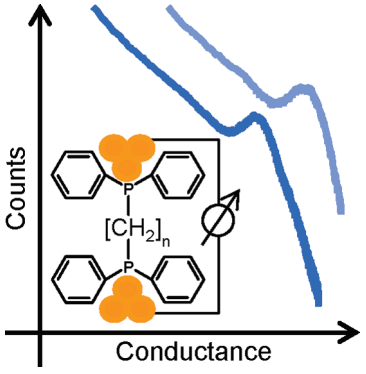

The development of molecular-scale electronics hinges on understanding the charge transport properties of single molecules.[1] A molecular junction consists of a molecule bound between two electrodes via terminal functional groups that link the molecule both electronically and mechanically.[2−5] The measured conductance of the trapped molecule depends not only on the molecular junction structure, but also on the choices of the electrode metal and the chemical link group. Together, these control both the junction mechanics as well as the electronic level alignment between the metal and molecule.[6,7] However, when some common link groups, such as thiols, are used with gold electrodes, the conductance varies significantly from junction to junction.[8−10] In contrast, link groups, such as amines,[11] methyl sulfides, or dimethyl phosphines,[4] which bind selectively to under-coordinated gold atoms, substantially reduce junction variability. This enables experiments that systematically compare electron transport across a range of related molecules.[7,9,12,13] Density functional theory (DFT)-based calculations have shown that amines and methyl sulfides have a relatively low binding energy (approximately 0.6 eV) to under-coordinated gold atoms.[4] While this is sufficient for transport measurements using the break-junction technique, such link groups are not ideal if prolonged mechanical junction stability is required. In contrast, dimethylphosphines were found to bind more strongly to gold, with a binding energy of approximately 1.2 eV. Unfortunately, dimethylphosphine-terminated molecules were relatively unstable and highly reactive under ambient conditions. This severely limited the variety of molecules that could be synthesized and measured with dimethylphosphine linkers.

Many advanced single molecule junction experiments would be enabled by a link group that combines the selectivity needed for junction formation with reproducible conductance and mechanical stability over a period of hours under various laboratory conditions. Here, we take a significant step toward achieving this goal by showing that diphenylphosphine (PPh_2) terminal groups, which are air stable, prove to be reliable chemical link groups that can successfully bind alkanes to gold electrodes. We measure the conductances of a series of PPh_2-terminated alkanes with 2−8 carbons in the backbone using the scanning tunneling microscope (STM)-based break-junction method. Conductance histograms constructed without any data selection from thousands of conductance versus displacement traces reveal clear peaks at conductance values that decrease exponentially with increasing molecule length. These data are fit to determine a tunneling decay constant, β,

Received Date: May 18, 2010
Accepted Date: June 16, 2010

DOI: 10.1021/jz100656s | *J. Phys. Chem. Lett.* **2010**, *1*, 2114–2119

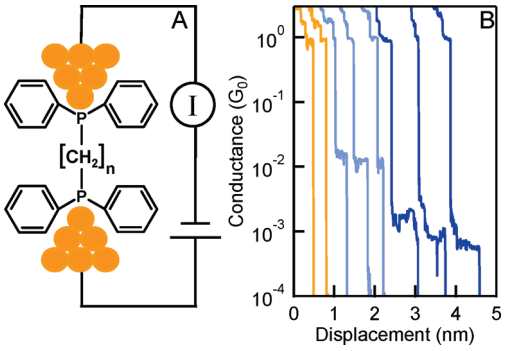

Figure 1. (A) A schematic of a single-molecule junction formed using PPh_2 linkers. (B) Sample conductance traces for clean gold (yellow), PPh_2E (light blue) ,and PPh_2P (dark blue) shown on a semilog plot. The traces are plotted against piezo displacement and offset horizontally for clarity. Measurements shown here are all made with a 25 mV bias at room temperature and in ambient conditions.

of 0.98 ± 0.04 per methylene (CH_2) group, which is comparable to that of the dimethylphosphine-terminated analogues.[4] Additionally, we find that the junction elongation length that can be sustained by PPh_2 linkers is very similar to that of the dimethylphosphine,[14] suggesting that the added steric bulk around the phosphine does not significantly alter single-molecule junction conductance, formation, or evolution. DFT-based calculations show relatively strong donor−acceptor bond formation to undercoordinated gold atoms, supporting this picture. Measured conductance histograms for four unsaturated PPh_2-linked molecules (benzene, acetylene, *cis*- and *trans*-ethylene) are much broader, with less well-defined peaks. We calculate the tunnel coupling for four of the alkanes and for the benzene-linked PPh_2 and find trends that correlate well with measurements.

Single-molecule junctions are formed using the STM-based break junction technique by repeatedly rupturing a gold point contact in a solution of target molecules as described in the Experimental and Theoretical Methods section below. Current is measured at a fixed bias as the junction is elongated past the point where the single molecule junction ruptures (Figure 1A). Representative traces showing conductance (current/voltage) versus sample displacement are shown in Figure 1B for three cases: clean gold with no analyte molecules, 1,2-bis(diphenylphosphino)ethane (PPh_2E), and 1,5-bis(diphenylphosphino)-pentane (PPh_2P). While in the reference (blank) case no signature, other than background tunneling, is observed after the single atom point-contact, with a conductance of 1 G_0 (= $2e^2/h$), is broken, the traces with analyte molecules present often show a signature step in the conductance trace.

In Figure 2A, we show conductance histograms created from more than 20 000 conductance traces for each PPh_2-terminated alkane. Clear conductance peaks are seen for all of the alkanes in this series, although for 1,4-bis(diphenylphosphino)-butane, the peak is quite broad, for reasons that are not yet clear to us. Lorentzian fits to these peaks are used to determine the most-probable value of molecular junction conductance. In Figure 2B, we show the peak positions plotted against carbon chain length on a semilog scale, along with an exponential fit to the data. The tunneling decay constant, β,

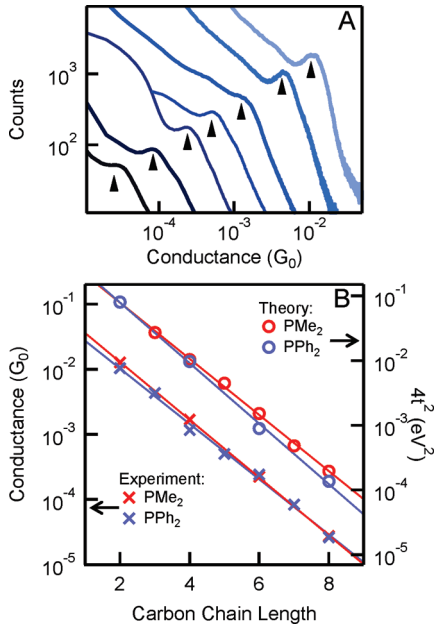

Figure 2. (A) Conductance histograms for seven PPh_2-linked alkanes ranging in length from two (right most curve, lightest blue) to eight (leftmost curve, darkest blue) methylene groups in the chain. Conductance measurements are made with a 25 mV bias for ethane through hexane and with a 100 mV for heptane and octane. Each histogram is constructed from over 20 000 conductance traces and plotted on a log−log scale. Histograms are normalized by the number of traces used to construct each histogram. The curves are offset vertically for clarity. Lorentzian fits are used to determine the peak positions (indicated by the arrows). The bin size is 10^{-5} G_0 for all measurements except for octane, where it is 10^{-6} G_0. (B) Conductance peak positions for PPh_2 (blue ×) and PMe_2 (red ×) linked alkanes obtained from Lorentzian fits to the histograms, plotted against carbon chain length, on a semilog plot (left axis). An exponential decrease in conductance is observed with increase in carbon chain length with a decay constant β = 0.98 ± 0.04 for the PPh_2 linker and 1.02 ± 0.04 for the PMe_2 linker. The square of the calculated tunnel coupling, $4t^2$ is also plotted against the number of methylene groups for both PPh_2 (blue ○) and PMe_2 (red ○) linkers. The calculated decay β values are 1.07 and 1.00, respectively.

determined from the fit ($G_N \sim e^{-\beta N}$) is 0.98 ± 0.04 per methylene group for this series. We also reproduce, in Figure 2B, conductance values for alkanes with 2, 4, 6, and 8 carbons terminated with PMe_2 linkers for comparison.[4] By extending the fit to the origin (N = 0), we determine effective contact resistance for two Ph_2P−Au bonds to be ∼180 kΩ. This value is close to that found for PMe_2 linkers, as can be seen in Figure 2B, indicating that the electronic coupling between the P and Au is similar for both link groups.

To investigate the nature of the bonding of a PPh_2 link group to under-coordinated gold, we performed DFT-based calculations as detailed below in the Experimental and Theoretical Methods section. We consider a series of PPh_2-terminated alkanes with 2, 4, 6, and 8 carbons, as well as for PMe_2-terminated alkanes with 3−8 carbons, bound to Au clusters representing the electrode on each side. We find that a donor−acceptor bond is formed through the delocalization of the lone pair on the phosphorus in PPh_2 and PMe_2 to an undercoordinated gold atom as we had previously shown for

DOI: 10.1021/jz100656s | J. Phys. Chem. Lett. 2010, 1, 2114–2119

the PMe_2 link group.[4] We find that the Au−PPh_2 bond has a binding energy of about 1 eV across this series, similar to that found in a study of PPh_3-stabilized Au_{20} clusters.[15] This binding energy is slightly lower than that of the PMe_2 linker, but considerably higher than that of an amine or methyl sulfide−Au bond.[4] To probe the electronic coupling through the junction using the DFT calculations, we extract a simplified donor−bridge−acceptor complex out of the cluster model, consisting of a single Au atom bonded to the molecule on each end. As described in the Experimental and Theoretical Methods section, the splitting, $2t$, between the highest occupied and lowest unoccupied molecular orbitals of this complex gives a quantitative estimate of this tunnel coupling between the donor and acceptor. In Figure 2B, we plot $4t^2$, which is proportional to the molecule conductance,[11,16−18] against the number of methylene groups for both linkers and determine a calculated β of 1.07 and 1.00 for the PPh_2 and PMe_2 linkers, respectively.

In order to understand how the junction evolves as it is elongated, we focus on the displacement information, in addition to conductance, using two-dimensional (2D) histograms. Individual conductance traces show plateaus at a molecule-dependent conductance value, with a length that corresponds to the distance a junction can be elongated before it is broken. When a junction breaks, it does so at the weakest link, which could be either at the molecule−gold bond or between the apex atom and the rest of the electrode. In order to determine the average distance a single-molecule junction can be extended before the junction breaks, we look at 2D histograms (see Experimental and Theoretical Methods section for details). In Figure 3A,B, we can see that conductance step length increases as the number of backbone carbons increases, as shown here for PPh_2E and PPh_2P, which have two and five carbons, respectively. From each histogram we determine a step length distribution by integrating the 2D histogram over half a decade in conductance centered at the molecular conductance peak, as indicated by the boxes in Figure 3A,B. To define the "longest step" length (characteristic of a junction whose final orientation is close to the stretching direction), we determine the length at which the distribution drops to 20% of its peak value for each molecule measured (upper panels, marked by an "×") and plot this in Figure 3C as a function of the number of methylene groups in the chain. A linear trend is observed with the "longest step" length increasing by ∼0.8 Å per carbon added, which is slightly less than the change in molecular length. This could be because the Au−Au vector in the Au−molecule−Au junction is not necessarily parallel to the stretching direction in every trace, thereby introducing variability in the elongation distances measured. Furthermore, this suggests that for junction formation, as illustrated in Figure 3D, short molecules insert with the link groups bonded near the apex atom of the tip and substrate, while long molecules can bind further away from one (or both) apex atoms. Because of this, we expect longer molecules to be able to access a larger number of binding sites, simply because of the greater number of under-coordinated gold atoms in the electrode available given the molecule length. Once a junction is formed, upon elongation, either the binding

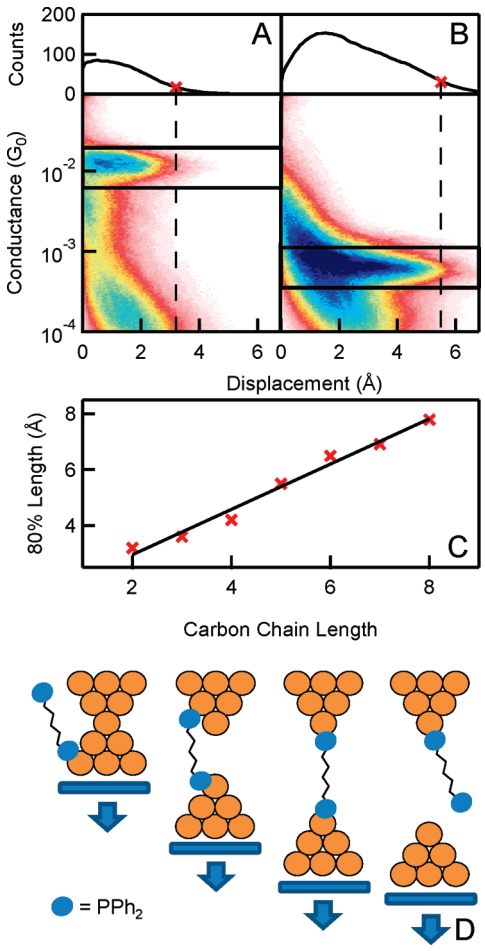

Figure 3. Examples of normalized 2D conductance versus displacement histograms of (A) PPh_2E and (B) PPh_2P, each made with 10 000 traces. In each, a conductance window of 0.5 decades centered around the peak conductance values is shown. Step length distributions (top panels) are obtained by summing over the conductance window shown. A "longest step" length has been determined for each molecule by locating the point at which the step length distribution falls to 20% of the maximal value, as indicated here by "×"s. (C) "Longest step" length plotted against the number of methylene groups in the chain along with a linear fit to the data. (D) Schematic depiction of junction elongation for PPh_2P. As the electrodes are pulled apart, the gold point contact breaks, and current can be measured through PPh_2P. Longer molecules have access to a larger number of binding sites along the gold electrode and can bridge the junction for greater elongation distances than shorter molecules.

site moves from one atom to the next or the gold electrodes deform under the pulling force.[14] Although gauche defects in alkanes are relatively low energy, meaning bent or folded conformations could bind at the apex,[19] in such cases, the junction conductance would initially be significantly lower, contrary to what we observe in the 2D histograms.[20]

These calculations and measurements suggest very strongly that the Ph_2P−Au bond is electronically well-coupled to the alkane backbone since the measurements yield narrow distributions in conductance. To investigate the coupling of the Ph_2P−Au bond to a conjugated backbone, we have also measured the conductance of four other molecules:

DOI: 10.1021/jz100656s | J. Phys. Chem. Lett. 2010, 1, 2114–2119

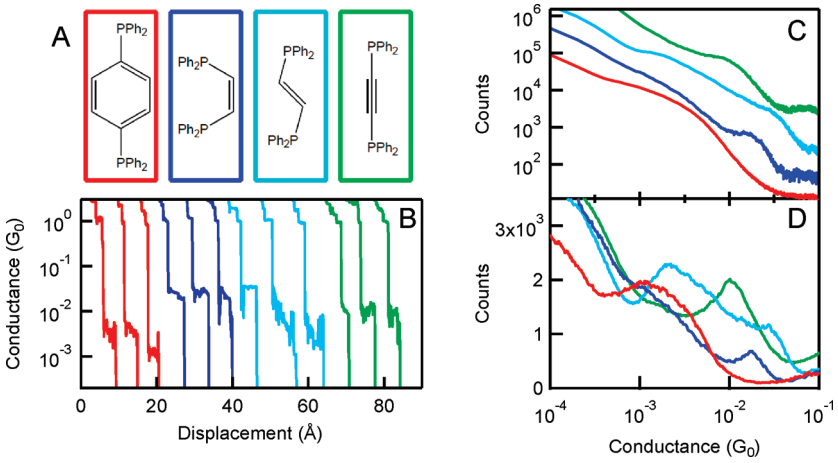

Figure 4. (A) Structures of four conjugated molecules with PPh_2 linkers: PPh_2B, (red), $cPPh_2E$ (dark blue), $tPPh_2E$, (light blue), and PPh_2A, (green). (B) Sample conductance versus displacement traces of the four molecules shown on a semilog plot. All data were measured at 25 mV bias at room temperature in ambient conditions. (C) Normalized linear-binned conductance histograms made from at least 5000 traces for each molecule plotted on a log−log scale. The histograms were all constructed with a bin size of 10^{-5} G_0. (D) Normalized log-binned histograms for the same molecules constructed from the same traces using 100 bins per decade of G_0.

1,4-bis(diphenylphosphino)benzene (PPh_2B), 1,2-bis(diphenylphosphino)acetylene (PPh_2A), *trans*-1,2-bis(diphenylphosphino)ethylene ($tPPh_2E$), and *cis*-1,2-bis(diphenylphosphino)-ethylene ($cPPh_2E$) (See Figure 4A for structures). Figure 4B shows sample conductance traces obtained from measurements of each of these four molecules in 1,2,4-trichlorobenzene. In Figure 4C, we show the conductance histograms constructed without any data selection from more than 5000 traces for each molecule using linear conductance bins, and in Figure 4D we show histograms constructed with the same traces using logarithmic conductance bins. First, we note that none of the linear-binned histograms in Figure 4C show clear peaks as compared to the results for alkanes (Figure 2B). Second, log-binned histograms (Figure 4D) show very broad peaks, indicating that junctions are indeed formed and that these molecules do conduct. This broad spread in measured conductance indicates that the electronic coupling across the molecules probably varies from junction to junction when the PPh_2 linker is attached to a conjugated backbone. This could occur if the Au−P bond in these molecular junctions is not as strongly coupled to the π-system in these molecules as, for example, the Au−N bonds are in the NH_2-terminated analogs.[21] To understand the origin of this variability, we focus on PPh_2B and perform DFT-based calculations of tunnel coupling as a function of the Au−P−C−C torsional angle as illustrated in Figure 5A. We find that the lowest energy conformation has a torsional angle of 135°. Thus, the coupling to the π-system is nominally reduced from its maximal value by a factor of 2 on both sides of the junction (one generally expects a $\cos^4\theta$ law for this case, where θ is the angle relative to the π-system, not the torsional Au−P−C−C angle). Furthermore, we find that this torsional angle can be changed by ±30° with an energy cost of less than 0.1 eV. However, the tunnel coupling changes by more than an order of magnitude (from about 0.001 eV^2 to 0.04 eV^2) within this range of accessible torsional angles, explaining the large spread in conductance

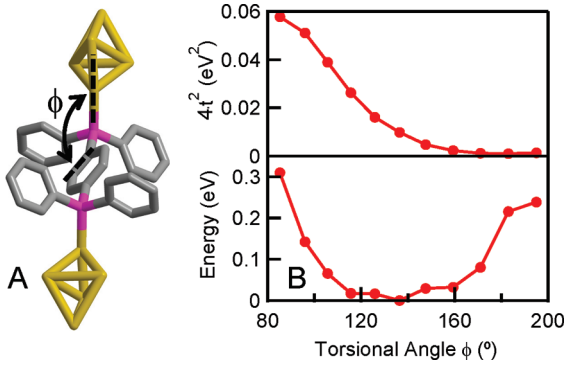

Figure 5. (A) Illustration of the Au−P−C−C torsional angle sampled for PPh_2B. (B) Lower panel: Plot of energy vs torsional angle for PPh_2B attached to Au_5 clusters indicating an energy minimum at 135°. Upper panel: Square of calculated tunnel coupling, $4t^2$, through PPh_2B attached to Au_1 clusters for the same range of torsional angles. The tunnel coupling changes by more than an order of magnitude within the range of accessible torsional angles.

measured for this molecule. The calculated tunnel coupling for PPh_2B at its energy minimum configuration is comparable to that of 1,4-bis(diphenylphosphino)butane, in agreement with experiment, where the conductances for PPh_2B and 1,4-bis(diphenylphosphino)butane are similar, comparing Figures 2A and 4D. Evidently, the conductance of PPh_2B bound in a configuration where the torsional angles are 0 is much lower than that of 1,4-bis(diphenylphosphino)butane.

The conductance histograms for the other three unsaturated molecules are considerably narrower than that of PPh_2B, consistent with the fact that one would expect higher rotation barriers for both the acetylene and ethylene molecules. However, unlike PPh_2E, none show a clear conductance peak. This is probably because the lone pair on the P is not aligned with the π-system of the lowest energy conformation of the ethylene and acetylene backbone, and thus even small

DOI: 10.1021/jz100656s | J. Phys. Chem. Lett. 2010, 1, 2114–2119

changes in the Au−P−C−C torsional angle would result in large changes in conductance. Temperature-dependent conductance measurements, which are beyond the scope of this work, would be required to probe this aspect further.

In summary, we have measured the conductance of seven PPh_2-terminated saturated alkanes and four PPh_2-terminated unsaturated molecules. The well-defined peaks in the conductance histograms suggest that the PPh_2 linker couples well into the σ-system. This indicates that the donor−acceptor bond of the PPh_2 linker is both selective and well-defined. We further find that the PPh_2 linkers do not couple as well to the π-system in conjugated molecules due to the orientation of the P lone-pair relative to the conjugated backbone. However, we propose that measuring specially designed molecules where the rotation along the P−C bond is restricted, thereby orienting the lone-pair along the π-system, would result in clear molecular signatures in conductance histograms.

EXPERIMENTAL AND THEORETICAL METHODS

We measure the conductance of a series of PPh_2-terminated molecules in a home-built modified STM that has been described previously.[11] Briefly, a gold tip (Alfa Aesar, 99.999%) is brought in and out of contact with a gold-on-mica substrate in an ~1 mM solution of the target molecule in 1,2,4-trichlorobenzene (Aldrich, 99.5%). All molecules were obtained commercially and further purified by recrystallization from appropriate solvents. 1,7-bis(diphenylphosphino)heptane and 1,4-bis(diphenylphosphino)benzene were synthesized according to literature procedures.[22,23] A gold point-contact is first formed, and, as it is broken, a molecule can be trapped between the broken ends to form a single-molecule junction (Figure 1A). The junction conductance (current/voltage) is measured at a constant applied bias of 25−100 mV as a function of the sample displacement (while the tip is held fixed), resulting in a conductance trace (Figure 1B). Typical conductance traces show steps at integer multiples of the quantum of conductance, $G_0 = 2e^2/h \approx 77.5\ \mu S$, a step at a molecule-dependent value below G_0, and sometimes a background due to tunneling across the gap between the electrodes (Figure 1B). For the displacement rates used, each conductance trace shown spans less than 100 ms. Since successive conductance traces are not identical, and since molecules are not trapped in every trace, thousands of conductance traces are collected. The data points of all the measured traces are compiled into a histogram of conductance for a statistical analysis, using linear conductance bins as shown in Figures 2A and 4C, and with logarithmic bins in Figure 4D. Peaks in the linear-binned histograms result when a significant fraction of all measured traces show plateaus at a narrow conductance range. When no molecules are present, the conductance histogram shows a background due to tunneling with histogram counts increasing with decreasing conductance.

2D conductance-displacement histograms are created from conductance traces for all molecules by first aligning all traces at the point where the Au−Au bond breaks, and then binning the data using linear bins along the displacement axis and logarithm bins along the conductance axis for image clarity.[14,24]

The DFT-based studies were performed using the generalized gradient approximation (GGA) as formulated by Perdew, Burke, and Ernzerhof (PBE).[25] The molecular calculations were done with Jaguar v7.5 using a 6-31g** basis for the light atoms and a lacvp** basis for Au.[26,27] Each PPh_2−Au link was modeled using Au clusters. On the basis of previous experience,[4] we use a five-atom Au cluster to simulate an undercoordinated Au contact atom on a close-packed Au contact, as illustrated in Figure 5A. Four Au atoms are frozen in a fragment of the face-centered cubic (fcc) packing arrangement from metallic Au, and an unconstrained Au atom is initially located in the environment of a hexagonal close-packed (hcp) hollow site on a Au(111) facet. As was done previously,[4] the junction elongation process is modeled by separating the frozen Au atoms representing the tip and substrate in 0.4 Å steps, allowing all other atoms to relax. In contrast to the experience with dimethylphosphine link groups, for some cases an attraction between the phenyl side groups of the PPh_2 linker and the corner atoms of the Au_5 cluster are observed in the relaxation. While this did not affect the results for the alkanes, for the case of PPh_2B, additional torsion angle constraints were utilized to control the position of the pendant phenyl groups. However, for the other conjugated molecules considered, reliable structures were not obtained. The minimum energy geometry from the junction elongation simulation is used for further study. To estimate the tunnel coupling for each molecule studied, the molecule plus the contact Au atom on each model electrode is extracted. The frontier orbitals (highest occupied and lowest unoccupied) of the Au−molecule−Au complex correspond to bond and antibonding combinations of the Au s-orbital on each side of the junction, tunnel coupled through the molecule. The splitting, denoted by $2t$ here, provides a quantitative estimate of the tunnel coupling.[7,16,18]

AUTHOR INFORMATION

Corresponding Author:

*To whom correspondence should be addressed. E-mail: mhyberts@bnl.gov (M.S.H.); lv2117@columbia.edu (L.V.).

ACKNOWLEDGMENT This work was supported in part by the Nanoscale Science and Engineering Initiative of the NSF (Award CHE-0641523), the New York State Office of Science, Technology, and Academic Research (NYSTAR), and NSF Career Award CHE-07-44185 (R.P. and L.V.). L.V. thanks ACS for PRF grant. This work was supported in part by the U.S. Department of Energy, Office of Basic Energy Sciences, under Contract Number DE-AC02-98CH10886 (M.S.H.).

REFERENCES

(1) Joachim, C.; Ratner, M. A. Molecular Electronics: Some Views on Transport Junctions and Beyond. *Proc. Natl. Acad. Sci. U.S.A.* **2005,** *102*, 8801–8808.
(2) Reed, M. A.; Zhou, C.; Muller, C. J.; Burgin, T. P.; Tour, J. M. Conductance of a Molecular Junction. *Science* **1997,** *278*, 252–254.
(3) Xu, B. Q.; Tao, N. J. J. Measurement of Single-Molecule Resistance by Repeated Formation of Molecular Junctions. *Science* **2003,** *301*, 1221–1223.

DOI: 10.1021/jz100656s | *J. Phys. Chem. Lett.* **2010,** *1*, 2114–2119

(4) Park, Y. S.; Whalley, A. C.; Kamenetska, M.; Steigerwald, M. L.; Hybertsen, M. S.; Nuckolls, C.; Venkataraman, L. Contact Chemistry and Single-Molecule Conductance: A Comparison of Phosphines, Methyl Sulfides, and Amines. *J. Am. Chem. Soc.* **2007,** *129*, 15768–15769.
(5) Kiguchi, M.; Tal, O.; Wohlthat, S.; Pauly, F.; Krieger, M.; Djukic, D.; Cuevas, J. C.; van Ruitenbeek, J. M. Highly Conductive Molecular Junctions Based on Direct Binding of Benzene to Platinum Electrodes. *Phys. Rev. Lett.* **2008,** *101*, 046801.
(6) Engelkes, V. B.; Beebe, J. M.; Frisbie, C. D. Length-Dependent Transport in Molecular Junctions Based on SAMs of Alkanethiols and Alkanedithiols: Effect of Metal Work Function and Applied Bias on Tunneling Efficiency and Contact Resistance. *J. Am. Chem. Soc.* **2004,** *126*, 14287–14296.
(7) Hybertsen, M. S.; Venkataraman, L.; Klare, J. E.; Whalley, A. C.; Steigerwald, M. L.; Nuckolls, C. Amine-Linked Single-Molecule Circuits: Systematic Trends across Molecular Families. *J. Phys.: Condens. Matter* **2008,** *20*, 374115.
(8) Ulrich, J.; Esrail, D.; Pontius, W.; Venkataraman, L.; Millar, D.; Doerrer, L. H. Variability of Conductance in Molecular Junctions. *J. Phys. Chem. B* **2006,** *110*, 2462–2466.
(9) Li, C.; Pobelov, I.; Wandlowski, T.; Bagrets, A.; Arnold, A.; Evers, F. Charge Transport in Single Au | Alkanedithiol | Au Junctions: Coordination Geometries and Conformational Degrees of Freedom. *J. Am. Chem. Soc.* **2008,** *130*, 318–326.
(10) Li, X. L.; He, J.; Hihath, J.; Xu, B. Q.; Lindsay, S. M.; Tao, N. J. Conductance of Single Alkanedithiols: Conduction Mechanism and Effect of Molecule−Electrode Contacts. *J. Am. Chem. Soc.* **2006,** *128*, 2135–2141.
(11) Venkataraman, L.; Klare, J. E.; Tam, I. W.; Nuckolls, C.; Hybertsen, M. S.; Steigerwald, M. L. Single-Molecule Circuits with Well-Defined Molecular Conductance. *Nano Lett.* **2006,** *6*, 458–462.
(12) Mishchenko, A.; Vonlanthen, D.; Meded, V.; Burkle, M.; Li, C.; Pobelov, I. V.; Bagrets, A.; Viljas, J. K.; Pauly, F.; Evers, F..; et al. Influence of Conformation on Conductance of Biphenyl-Dithiol Single-Molecule Contacts. *Nano Lett.* **2010,** *10*, 156–163.
(13) Akkerman, H. B.; de Boer, B. Electrical Conduction through Single Molecules and Self-Assembled Monolayers. *J. Phys.: Condens. Matter* **2008,** *20*, 013001.
(14) Kamenetska, M.; Koentopp, M.; Whalley, A.; Park, Y. S.; Steigerwald, M.; Nuckolls, C.; Hybertsen, M.; Venkataraman, L. Formation and Evolution of Single-Molecule Junctions. *Phys. Rev. Lett.* **2009,** *102*, 126803.
(15) Zhang, H.-F.; Stender, M.; Zhang, R.; Wang, C.; Li, J.; Wang, L.-S. Toward the Solution Synthesis of the Tetrahedral Au_{20} Cluster. *J. Phys. Chem. B* **2004,** *108*, 12259–12263.
(16) Woitellier, S.; Launay, J. P.; Joachim, C. The Possibility of Molecular Switching - Theoretical Study of $[(NH_3)5Ru\text{-}4,4'\text{-}bipy\text{-}Ru(NH_3)5]5^+$. *Chem. Phys.* **1989,** *131*, 481–488.
(17) Venkataraman, L.; Klare, J. E.; Nuckolls, C.; Hybertsen, M. S.; Steigerwald, M. L. Dependence of Single-Molecule Junction Conductance on Molecular Conformation. *Nature* **2006,** *442*, 904–907.
(18) Mcconnell, H. Intramolecular Charge Transfer in Aromatic Free Radicals. *J. Chem. Phys.* **1961,** *35*, 508–515.
(19) Haiss, W.; Wang, C. S.; Grace, I.; Batsanov, A. S.; Schiffrin, D. J.; Higgins, S. J.; Bryce, M. R.; Lambert, C. J.; Nichols, R. J. Precision Control of Single-Molecule Electrical Junctions. *Nat. Mater.* **2006,** *5*, 995–1002.
(20) Jones, D. R.; Troisi, A. Single Molecule Conductance of Linear Dithioalkanes in the Liquid Phase: Apparently Activated Transport Due to Conformational Flexibility. *J. Phys. Chem. C* **2007,** *111*, 14567–14573.
(21) Park, Y. S.; Widawsky, J. R.; Kamenetska, M.; Steigerwald, M. L.; Hybertsen, M. S.; Nuckolls, C.; Venkataraman, L. Frustrated Rotations in Single-Molecule Junctions. *J. Am. Chem. Soc.* **2009,** *131*, 10820–10821.
(22) Honaker, M. T.; Sandefur, B. J.; Hargett, J. L.; McDaniel, A. L.; Salvatore, R. N. CsOH-Promoted P-Alkylation: A Convenient and Highly Efficient Synthesis of Tertiary Phosphines. *Tetrahedron Lett.* **2003,** *44*, 8373–8377.
(23) Allen, D. V.; Venkataraman, D. Copper-Catalyzed Synthesis of Unsymmetrical Triarylphosphines. *J. Org. Chem.* **2003,** *68*, 4590–4593.
(24) Martin, C. A.; Ding, D.; Sorensen, J. K.; Bjornholm, T.; van Ruitenbeek, J. M.; van der Zantt, H. S. J. Fullerene-Based Anchoring Groups for Molecular Electronics. *J. Am. Chem. Soc.* **2008,** *130*, 13198–13199.
(25) Perdew, J. P.; Burke, K.; Ernzerhof, M. Generalized Gradient Approximation Made Simple. *Phys. Rev. Lett.* **1996,** *77*, 3865–3868.
(26) *Jaguar 7.5*; Schrodinger, L.L.C.: New York, 2008.
(27) Wadt, W. R.; Hay, P. J. Abinitio Effective Core Potentials for Molecular Calculations - Potentials for Main Group Elements Na to Bi. *J. Chem. Phys.* **1985,** *82*, 284–298.

DOI: 10.1021/jz100656s | *J. Phys. Chem. Lett.* **2010,** *1*, 2114–2119